Phanerozoic variation in dolomite abundance linked to oceanic anoxia

Mingtao Li[1,2], Paul B. Wignall[3], Xu Dai[2], Mingyi Hu[1] and Haijun Song[2]*

[1]School of Geosciences, Yangtze University, Wuhan 430100, China
[2]State Key Laboratory of Biogeology and Environmental Geology, School of Earth Sciences, China University of Geosciences, Wuhan 430074, China
[3]School of Earth and Environment, University of Leeds, Leeds LS29JT, UK

ABSTRACT

The abundance of dolomitic strata in the geological record contrasts with the general rarity of locations where dolomite forms today, a discrepancy that has long posed a problem for their interpretation. Recent culture experiments show that dolomite can precipitate at room temperature, raising the possibility that many ancient dolomites may be of syngenetic origin. We compiled a large geodata set of secular variations in dolomite abundance in the Phanerozoic, coupled with compilations of genus richness of marine benthic invertebrates and sulfur-isotope variations in marine carbonates. These data show that dolomite abundance is negatively correlated to genus diversity, with four dolomite peaks occurring during mass extinctions. Dolomite peaks also correspond to the rapid increase in sulfur-isotope composition (δ^{34}S), an indicator of enhanced sulfate reduction, in anoxic oceans. These results confirm that variations in dolomite abundance during the Phanerozoic were closely linked with changes in marine benthic diversity, with both in turn related to oceanic redox conditions.

INTRODUCTION

Dolomite is a form of rhombohedral carbonate mineral that is common in carbonate successions in the geological record, and it often forms dolostones, which can be important hydrocarbon reservoirs (e.g., Petrash et al., 2017). Research on dolomite formation can be divided into three stages (Burns et al., 2000): (1) the first stage (1800–1900 CE) was marked by the study of synthesis of dolomite at high temperature (250 °C); (2) the second stage (1900–1995) saw discoveries of dolomite in modern environments and the development of new models to explain dolomite formation; and (3) the third stage (1995–present) was characterized by series of experiments that showed dolomite could be synthesized at low temperatures in the presence of microbes. Current dolomite formation models include the mixing model (Folk and Land, 1975), the sabkha model (Wells, 1962), and recent microbial models (Vasconcelos et al., 1995; Bontognali et al., 2010). However, there remains a long-running debate on whether most

dolomite in the geological record formed during late burial diagenesis or syngenetically in the depositional environment.

We aimed to address this problem by compiling a large geodata set to show the secular variations in dolomite abundance during the Phanerozoic and to investigate factors that correlate with dolomite fluctuations. Previous research has linked dolomite abundance in the Phanerozoic Eon with fluctuations in atmospheric oxygen (Burns et al., 2000), sulfur-isotope composition (Burns et al., 2000; Li et al., 2018), and global eustasy (Sibley, 1991). The lack of a large dolomite geodata set has made evaluation of these and other links uncertain.

METHODS

In order to reveal the fluctuations of dolomite abundance in the Phanerozoic, we selected 1984 worldwide marine carbonate sections (see Dataset S1 in the Supplemental Material[1]) spanning from the Cambrian to Neogene to comprise a large geodata set. Study sections were compiled from the published literature). These sections represent a variety of ancient marine sedimen-

tary environments, ranging from shallow to deep seas, with ages well constrained by biostratigraphy and/or chemostratigraphy.

Dolomite abundance in Phanerozoic history is expressed here as the mean dolomite content (dolomite thickness / total carbonate thickness) in carbonate successions with a temporal resolution of epoch referenced to the 2019 CE international chronostratigraphic chart (International Commission on Stratigraphy, https://stratigraphy.org/ICSchart/ChronostratChart2019-05.pdf). Some epochs with much longer durations, e.g., early/late Carboniferous and Early/Late Cretaceous, were divided into two bins to improve the temporal resolution, with an average temporal accuracy of 15.8 ± 7.4 m.y. To minimize sampling bias, for each time bin, 45 sections per time bin from 8 to 21 countries (see Table S1) were randomly selected to perform a resampling process with 10,000 iterations in the R program (version 3.3.1, https://www.r-project.org), to calculate the average dolomite abundance with a 95% confidence interval. The dolomite abundance is reported here as the result of this resampling process, if not otherwise specified.

To investigate potential correlations of dolomite abundance, our data were compared with the reported occurrences of oceanic anoxic events, genus richness of marine benthic invertebrates, and the rate of change of δ^{34}S (see Tables S2 and S3); Spearman's analysis was performed using SPSS software (SPSS version 22.0, https://www.ibm.com/support/pages/spss-statistics-220-available-download/). Meanwhile, frequency and the Shapiro-Wilk test (normality test) were performed to check whether these variables were consistent with normal distributions (Figs. S1–S6). The rate of change of δ^{34}S
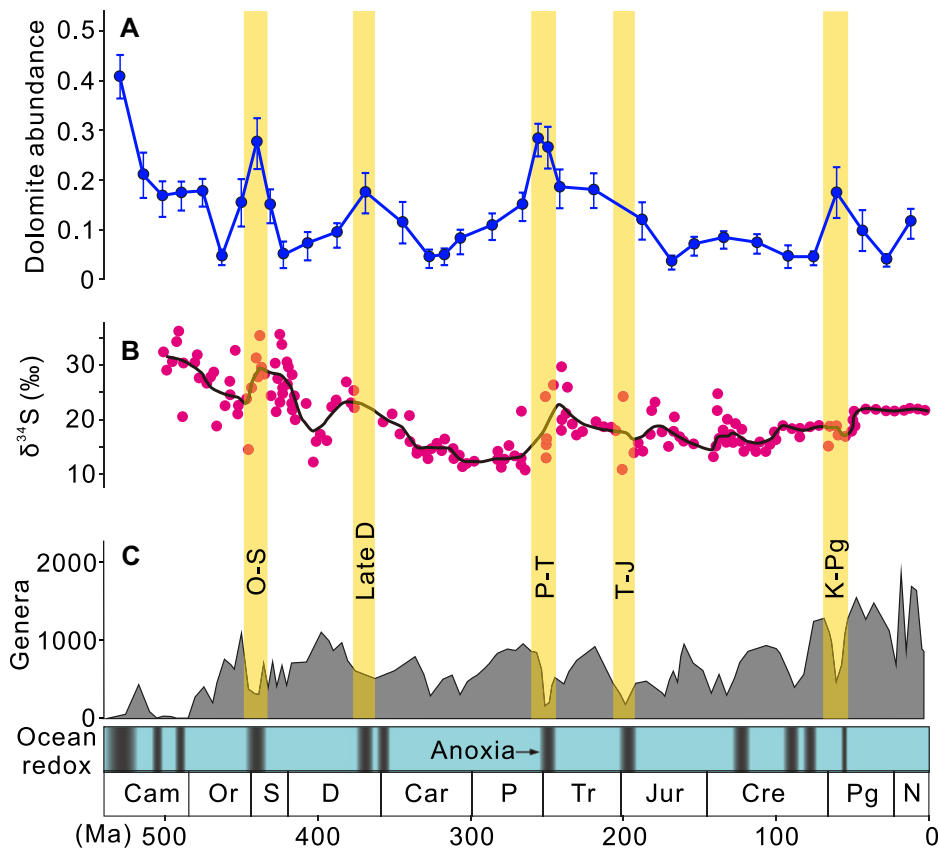
*E-mail: haijunsong@cug.edu.cn

Figure 1. Environmental and biotic variables related to Phanerozoic dolomite abundance. (A) Variations in dolomite abundance (results of 10,000 resampling runs) throughout the Phanerozoic. Blue dots indicate mean values, and error bars indicate 95% confidence interval. (B) Sulfur-isotope composition of Phanerozoic marine carbonate rocks. (C) Diversity of marine benthic invertebrates and oceanic redox conditions in Phanerozoic history. Yellow bars highlight five mass extinctions. Sulfur isotope data are from Kampschulte and Strauss (2004), Prokoph et al. (2008), and Hannisdal and Peters (2011); note that almost all sulfur isotope data (171 out of 186) are sourced from the same regions where carbonate sections presented in our geodata set are located (see Dataset S1 in the Supplemental Material [see footnote 1]; see also Kampschulte and Strauss, 2004). Paleontology data are from Paleobiology Database (PBDB; https://paleobiodb.org). Ocean anoxic events are from Whiteside and Grice (2016) and Song et al. (2017), with modifications. Cam—Cambrian; Or—Ordovician; S—Silurian; D—Devonian; Car—Carboniferous; P—Permian; Tr—Triassic; Jur—Jurassic; Cre—Cretaceous; Pg—Paleogene; N—Neogene.

$(R_{\delta^{34}S})$ and the mean $\bar{R}_{\delta^{34}S}$ for each time bin were calculated as

$$R_{\delta^{34}S_i} = \frac{\delta^{34}S_{i+1} - \delta S_i}{Age_i - Age_{i+1}}, \quad (1)$$

and

$$\bar{R}_{\delta^{34}S} = \frac{R_{\delta^{34}S_i} + R_{\delta^{34}S_{i+1}} + \ldots + R_{\delta^{34}S_{i+n-1}}}{n}. \quad (2)$$

RESULTS

Dolomite abundance in Phanerozoic history showed major fluctuations ranging from 0.04 ± 0.03 to 0.41 ± 0.05, with a mean value of 0.13 ± 0.03 ($n = 1,984$) (Fig. 1A). Initial abundance in the Cambrian was high (0.24 ± 0.05, $n = 222$), but there was a sharp decline from the earliest Cambrian peak value of 0.41 (± 0.05, $n = 53$) to 0.05 (± 0.02, $n = 53$) in the Middle Ordovician. The trend reversed sharply in the Late Ordovician and increased to 0.28 ± 0.04 ($n = 54$) in the early Silurian. Subsequently, dolomite abundance dropped to 0.05 ± 0.03 ($n = 66$) at the end of the Silurian, and then it rose once again to 0.18 ± 0.05 ($n = 62$) in the Late Devonian. The following Carboniferous was characterized by low dolomite abundance (0.07 ± 0.05, $n = 237$) with slight fluctuations. The Permian saw a significant increase in dolomite abundance that reached 0.28 ± 0.05 ($n = 111$) at the Permian-Triassic boundary. Dolomite abundance remained at high levels (0.21 ± 0.02, $n = 179$) throughout the Triassic. A significant decline in dolomite abundance occurred at the beginning of the Jurassic, and it then remained low (0.06 ± 0.02, $n = 348$) throughout the Middle Jurassic to Late Cretaceous. This nadir was punctuated by a high spike (0.18 ± 0.06, $n = 72$) at the Cretaceous-Paleogene boundary.

The Paleogene showed a gradual decrease in dolomite abundance from 0.18 ± 0.06 ($n = 72$) in the Paleocene to a 0.04 ± 0.02 ($n = 52$) low point in the Oligocene, followed by a slight increase up to 0.12 ± 0.04 ($n = 55$) at the Paleogene-Neogene transition.

The comparison of dolomite abundance with marine generic diversity showed an inverse relationship ($R^2 = 0.20$, $p = 0.007$; see Fig. 2A) with four high anomalies during mass extinction intervals (Fig. 1C). The highest value of dolomite abundance in the Phanerozoic occurred in the Terreneuvian (early Cambrian) when diversity was at its lowest level. Dolomite abundance subsequently showed four high values of 0.28 ± 0.04 ($n = 54$, Ordovician–Silurian), 0.18 ± 0.05 ($n = 62$, Late Devonian), 0.28 ± 0.05 ($n = 111$, Permian–Triassic), and 0.18 ± 0.04 ($n = 72$, Cretaceous–Paleogene), all of which correspond with mass extinctions intervals.

Phanerozoic dolomite abundance showed a similar correspondence with sulfur-isotope variations in marine carbonate rocks (Fig. 1B). Thus, in this record, there are four significant declines of dolomite abundance (late Cambrian to Early Ordovician, early Silurian to late Silurian, Late Devonian to middle Carboniferous, Early Triassic to Middle Jurassic), immediately followed by four sharp increases (Ordovician–Silurian, Late Devonian, Permian–Triassic, Cretaceous–Paleogene), which all correspond to sulfur-isotope changes and oceanic anoxic events. Therefore, the high dolomite abundances in the Phanerozoic show good correlation with oceanic anoxic events (Fig. 1), with the exception of the Cretaceous record of these phenomena.

DISCUSSION
Data Set and Results Evaluation

By analyzing selected sections from a global geodata set, we aimed to minimize the effect of regional depositional and/or diagenetic influences on the secular trends identified here. Carbonate minerals, including aragonite, calcite, and dolomite, are sensitive to local sedimentary and/or diagenetic conditions and can be easily transformed into another mineral phase during diagenesis. Therefore, regional geodata sets may not reflect global variations in dolomite abundance. Another advantage of a global geodata set is that the absence of carbonate rocks in a region, due to tectonic movements or rapid climate changes, can be offset by data from other regions to create a continuous geological record. Such carbonate absences include the Upper Ordovician to Middle Carboniferous stratigraphic gap in North China due to tectonism (Wang et al., 2010), and the paucity of carbonate rocks in North America since the end of the Permian (Peters, 2006). There are, however, some limitations to our data set and our results due to
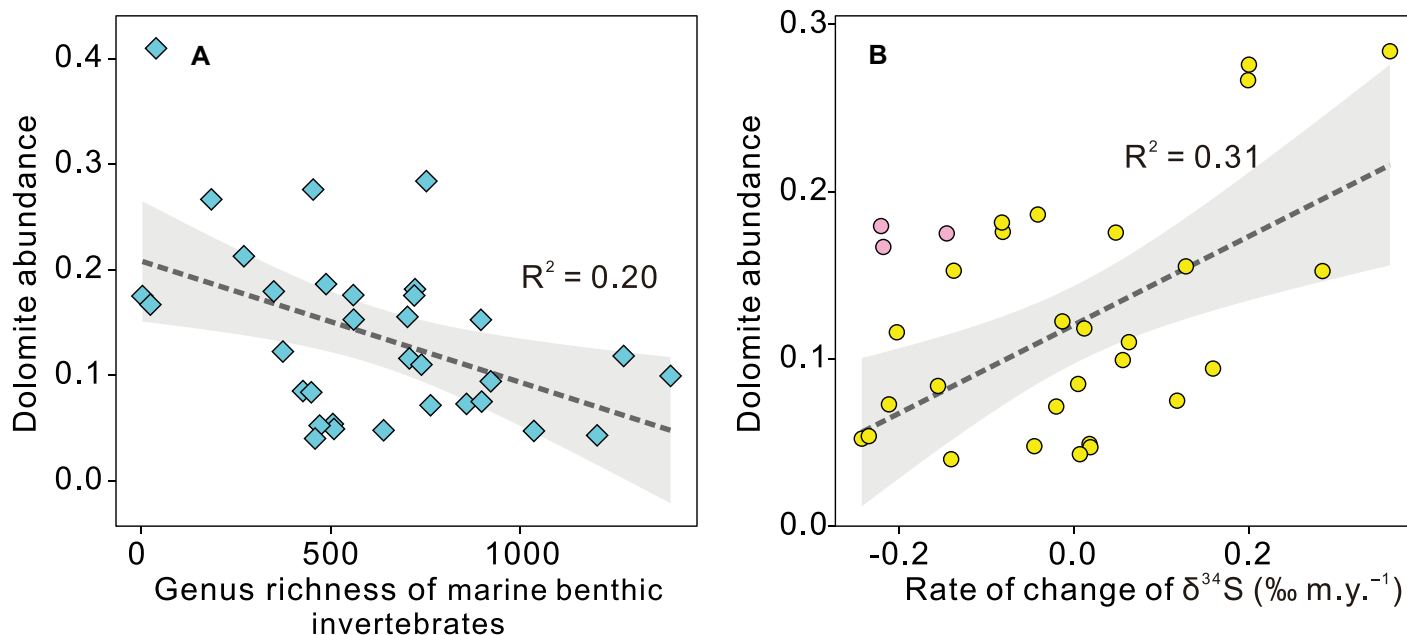
Figure 2. (A) Dolomite abundance versus genus richness of marine benthic invertebrates, showing negative correlation (p = 0.007). (B) Dolomite abundance versus rate of change of $\delta^{34}S$, showing positive correlation (p = 0.002) (pink dots spanning the middle Cambrian to Early Ordovician were excluded from analysis; see the Discussion in the text), where an increase in $\delta^{34}S$ is a good proxy of enhanced pyrite burial caused by intense sulfate reductions.

the relatively low temporal resolution of the dolomite abundance data, which may make it difficult to detect correlations with short-term environmental conditions, such as the Cretaceous oceanic anoxic events.

Origin of Phanerozoic Dolomites

There has been a long-running debate on whether Phanerozoic dolomites are predominantly syngenetic or the product of secondary dolomitization of other carbonates. The syngenetic alternative invokes dolomite nucleation and in situ stabilization within the water column or in pore waters during early diagenesis (Petrash et al., 2017). By contrast, secondary dolomites are thought to result from deep-burial dolomitization, a process whereby Mg^{2+} ions replace Ca^{2+} ions in calcite. It is often hard to tell whether dolomites are derived from syngenetic processes or later diagenesis using petrological observation and geochemical analysis, because most dolomites undergo recrystallization that alters their primitive textures and chemical signals (e.g., Land et al., 1975; Burns and Baker, 1987). However, it is worth noting that syngenetic and secondary processes occur in different environments, with the former in the biosphere and the latter in the lithosphere. So, the key to the origin of Phanerozoic dolomite might rely on the determination of the environment in which they formed.

The dolomite abundance in Phanerozoic history shows negative correlations with marine benthic invertebrate diversity, with four dolomite peaks coinciding with four mass extinctions. Only the Triassic-Jurassic mass extinction shows no obvious correlation

with a dolomite peak. It is noteworthy that the dolomite abundance in the Early Jurassic, following the Triassic-Jurassic mass extinction, is higher than the remaining period of the Jurassic, indicating a possible link between dolomite abundance and this biotic crisis. Previous studies have shown that the five mass extinctions in the Phanerozoic were accompanied by exceptional carbon- and sulfur-isotope excursions, indicating large perturbations of carbon and sulfur cycles through massive organic carbon burial and high pyrite burial due to intensive sulfate reductions under anoxic conditions (Stanley, 2010; Hannisdal and Peters, 2011). Therefore, the coupling between dolomite abundance and mass extinctions, with their associated environmental changes, suggests that Phanerozoic dolomites are most likely of syngenetic origin.

Controlling Factors for Phanerozoic Dolomites

The dolomite peaks in our analysis coincided with oceanic anoxic events, indicating that redox conditions may have been a key controlling factor. In normal conditions, oxygenated seafloor environments support a benthic community that includes a range of burrowing organisms, and their activities have a great impact on sediment biogeochemistry (e.g., Rosenberg et al., 2001; Weissberger et al., 2009). Intensive burrowing by benthos leads to the oxidization of shallow sediments and hinders microbial growth on the seabed and within shallow sediments (Fig. 3A). In contrast, intervals of widespread anoxia (e.g., at the Permian-Triassic boundary) result in the

demise of benthic fauna (Wignall and Twitchett, 2002) and the bloom of seabed microbes in the form of microbial mats (Fig. 3B) (Pruss et al., 2004). Oceanic anoxia also leads to intense anaerobic respiration, anoxygenic photosynthesis, and sulfate reduction and, consequently, the production of large amounts of HS^-, extracellular polymeric substances (EPS), and organic carbon carboxyl. The bloom of microbes and associated by-products, such as HS^- and organic carbon carboxyl, can efficiently promote syngenetic dolomite formation (Wright and Wacey, 2005; Zhang et al., 2012; Roberts et al., 2013; Bontognali et al., 2014; Bontognali, 2019). The discovery of syngenetic dolomite in modern anoxic environments (at Lagoa Vermelha, Brazil) supports this link (Vasconcelos and McKenzie, 1997). Dolostones were also widespread in the anoxic oceans that developed at the Permian-Triassic boundary, where they have been associated with abundant microbial relics such as EPS evidence and fossilized microbes (Li et al., 2018).

It was previously thought that the presence of sulfate inhibited dolomite formation. However, modern dolomite experiments have shown that dolomite can precipitate from solutions with high sulfate concentrations (up to 56 mM) when microbes are present, including both halophilic aerobic and sulfate-reducing types (Sánchez-Román et al., 2009; Deng et al., 2010). The sulfur-isotope record indirectly monitors the intensity of microbial sulfate reduction in oceans, because evidence shows that the burial of pyrite played a key role in Phanerozoic $\delta^{34}S$ patterns (Hannisdal and Peters, 2011; Bernasconi et al.,
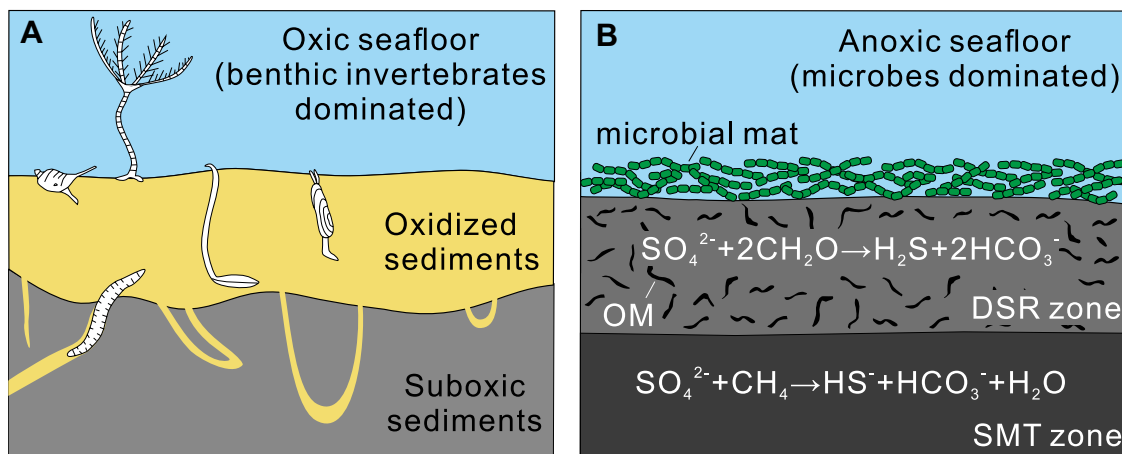
Figure 3. Schematic models of benthic community and redox conditions for oxic and anoxic seafloor environments. (A) Benthic invertebrates dominate seafloor under oxic conditions, and sediments are oxidized due to burrowing and irrigation by benthic invertebrates. (B) Microbes dominate seafloor under anoxic conditions. Seafloors are colonized by microbial mats that provide sufficient organic matter for underlying sediments to sustain intensive sulfate reduction. OM—organic matter, DSR—dissimilatory sulfate reduction, SMT—sulfate-methane transition.

2017). The rate of change in the $\delta^{34}S$ record since the Ordovician radiation is related to dolomite abundance ($R^2 = 0.31$, $p = 0.002$; Fig. 2B), with significant increases in $\delta^{34}S$ corresponding to dolomite peaks.

The broad-scale link between diversity and dolomite abundance is not seen for the minor declines of generic diversity. For example, low points of genus richness are seen in the middle Carboniferous, Middle Jurassic, and Cretaceous (and the latter is associated with ocean anoxia), but there are no coincident dolomite peaks. We would argue that these diversity changes were not linked to suppressed benthic activity on a global scale, which is likely the key factor in dolomite formation. In addition, the Cretaceous oceanic anoxic events may not have been sufficiently extensive to stimulate sufficient microbial production of by-products such as HS^- and EPS, which are essential for dolomite formation (McCormack et al., 2018).

Further work is still needed to corroborate the causal relationship between environmental factors and dolomite abundance. Mg/Ca ratios have been considered as the controlling factor in dolomite formation. However, efforts to synthesize dolomite in the laboratory under abiotic conditions with high Mg/Ca ratios close to 2 (levels that certainly exceed dolomite saturation) failed (Land, 1998). In contrast, dolomites were successfully synthesized in the laboratory in the presence of microbes with fairly low Mg/Ca ratios of 0.3 and 0.69 (Roberts et al., 2004; Kenward et al., 2009), suggesting that Mg/Ca ratios play a limited role in dolomite formation. The dolomite abundance in the Phanerozoic was probably affected by the combination of several environmental factors, such as genus richness, oceanic redox conditions, sulfate reduction rates, etc. A higher-temporal-resolution geodata set containing multiple environmental parameters might reveal additional correlations and further help to resolve the long-standing dolomite problem.

REFERENCES CITED
Bernasconi, S.M., Meier, I., Wohlwend, S., Brack, P., Hochuli, P.A., Bläsi, H., Wortmann, U.G., and Ramseyer, K., 2017, An evaporite-based high-resolution sulfur isotope record of late Permian and Triassic seawater sulfate: Geochimica et Cosmochimica Acta, v. 204, p. 331–349, https://doi.org/10.1016/j.gca.2017.01.047.

Bontognali, T.R.R., 2019, Anoxygenic phototrophs and the forgotten art of making dolomite: Geology, v. 47, p. 591–592, https://doi.org/10.1130/focus062019.1.

Bontognali, T.R.R., Vasconcelos, C., Warthmann, R.J., Bernasconi, S.M., Dupraz, C., Strohmengers, C.J., and McKenzie, J.A., 2010, Dolomite formation within microbial mats in the coastal sabkha of Abu Dhabi (United Arab Emirates): Sedimentology, v. 57, p. 824–844, https://doi.org/10.1111/j.1365-3091.2009.01121.x.

Bontognali, T.R.R., McKenzie, J.A., Warthmann, R.J., and Vasconcelos, C., 2014, Microbially influenced formation of Mg-calcite and Ca-dolomite in the presence of exopolymeric substances produced by sulphate-reducing bacteria: Terra Nova, v. 26, p. 72–77, https://doi.org/10.1111/ter.12072.

Burns, S.J., and Baker, P.A., 1987, A geochemical study of dolomite in the Monterey Formation, California: Journal of Sedimentary Research, v. 57, p. 128–139, https://doi.org/10.1306/212F8AC6-2B24-11D7-8648000102C1865D.

Burns, S.J., McKenzie, J.A., and Vasconcelos, C., 2000, Dolomite formation and biogeochemical cycles in the Phanerozoic: Sedimentology, v. 47, p. 49–61, https://doi.org/10.1046/j.1365-3091.2000.00004.x.

Deng, S., Dong, H., Lv, G., Jiang, H., Yu, B., and Bishop, M.E., 2010, Microbial dolomite precipitation using sulfate reducing and halophilic bacteria: Results from Qinghai Lake, Tibetan Plateau, NW China: Chemical Geology, v. 278, p. 151–159, https://doi.org/10.1016/j.chemgeo.2010.09.008.

Folk, R.L., and Land, L.S., 1975, Mg/Ca ratio and salinity: Two controls over crystallization of dolomite: AAPG Bulletin, v. 59, p. 60–68, https://doi.org/10.1306/83D91C0E-16C7-11D7-8645000102C1865D.

Hannisdal, B., and Peters, S.E., 2011, Phanerozoic Earth system evolution and marine biodiversity: Science, v. 334, p. 1121–1124, https://doi.org/10.1126/science.1210695.

Kampschulte, A., and Strauss, H., 2004, The sulfur isotopic evolution of Phanerozoic seawater based on the analysis of structurally substituted sulfate in carbonates: Chemical Geology, v. 204, p. 255–286, https://doi.org/10.1016/j.chemgeo.2003.11.013.

Kenward, P.A., Goldstein, R.H., Gonzalez, L.A., and Roberts, J.A., 2009, Precipitation of low-temperature dolomite from an anaerobic microbial consortium: The role of methanogenic Archaea: Geobiology, v. 7, p. 556–565, https://doi.org/10.1111/j.1472-4669.2009.00210.x.

Land, L.S., 1998, Failure to precipitate dolomite at 25 °C from dilute solution despite 1000-fold oversaturation after 32 years: Aquatic Geochemistry, v. 4, p. 361–368, https://doi.org/10.1023/A:1009688315854.

Land, L.S., Salem, M.R.I., and Morrow, D.W., 1975, Paleohydrology of ancient dolomites: Geochemical evidence: American Association of Petroleum Geologists Bulletin, v. 59, p. 1602–1625, https://doi.org/10.1306/83D9200F-16C7-11D7-8645000102C1865D.

Li, M., Song, H., Algeo, T.J., Wignall, P.B., Dai, X., and Woods, A.D., 2018, A dolomitization event at the oceanic chemocline during the Permian-Triassic transition: Geology, v. 46, p. 1043–1046, https://doi.org/10.1130/G45479.1.

McCormack, J., Bontognali, T.R.R., Immenhauser, A., and Kwiecien, O., 2018, Controls on cyclic formation of Quaternary early diagenetic dolomite: Geophysical Research Letters, v. 45, p. 3625–3634, https://doi.org/10.1002/2018GL077344.

Peters, S.E., 2006, Macrostratigraphy of North America: The Journal of Geology, v. 114, p. 391–412, https://doi.org/10.1086/504176.

Petrash, D.A., Bialik, O.M., Bontognali, T.R.R., Vasconcelos, C., Roberts, J.A., McKenzie, J.A., and Konhauser, K.O., 2017, Microbially catalyzed dolomite formation: From near-surface to burial: Earth-Science Reviews, v. 171, p. 558–582, https://doi.org/10.1016/j.earscirev.2017.06.015.

Prokoph, A., Shields, G.A., and Veizer, J., 2008, Compilation and time-series analysis of a marine carbonate $\delta^{18}O$, $\delta^{13}C$, $^{87}Sr/^{86}Sr$ and $\delta^{34}S$ database through Earth history: Earth-Science Reviews, v. 87, p. 113–133, https://doi.org/10.1016/j.earscirev.2007.12.003.

Pruss, S., Fraiser, M., and Bottjer, D.J., 2004, Proliferation of Early Triassic wrinkle structures: Implications for environmental stress following the end-Permian mass extinction: Geology, v. 32, p. 461–464, https://doi.org/10.1130/G20354.1.

Roberts, J.A., Bennett, P.C., González, L.A., Macpherson, G.L., and Milliken, K.L., 2004, Microbial precipitation of dolomite in methanogenic groundwater: Geology, v. 32, p. 277–280, https://doi.org/10.1130/G20246.2.

Roberts, J.A., Kenward, P.A., Fowle, D.A., Goldstein, R.H., González, L.A., and Moore, D.S., 2013, Surface chemistry allows for abiotic precipitation of dolomite at low temperature: Proceedings of the National Academy of Sciences of the United States of America, v. 110, p. 14540–14545, https://doi.org/10.1073/pnas.1305403110.

Rosenberg, R., Nilsson, H.C., and Diaz, R.J., 2001, Response of benthic fauna and changing sediment redox profiles over a hypoxic gradient: Estuarine, Coastal and Shelf Science, v. 53, p. 343–350, https://doi.org/10.1006/ecss.2001.0810.

Sánchez-Román, M., McKenzie, J.A., Wagener, A.de L.R., Rivadeneyra, M.A., and Vasconcelos, C., 2009, Presence of sulfate does not inhibit low-temperature dolomite precipitation: Earth and Planetary Science Letters, v. 285, p. 131–139, https://doi.org/10.1016/j.epsl.2009.06.003.

Sibley, D.F., 1991, Secular changes in the amount and texture of dolomite: Geology, v. 19, p. 151–154, https://doi.org/10.1130/0091-7613(1991)019<0151:SCITAA>2.3.CO;2.

Song, H., Jiang, G., Poulton, S.W., Wignall, P.B., Tong, J., Song, H., An, Z., Chu, D., Tian, L., and She, Z., 2017, The onset of widespread marine red beds and the evolution of ferruginous oceans: Nature Communications, v. 8, p. 1–7, https://doi.org/10.1038/s41467-017-00502-x.

Stanley, S.M., 2010, Relation of Phanerozoic stable isotope excursions to climate, bacterial metabolism, and major extinctions: Proceedings of the National Academy of Sciences of the United States of America, v. 107, p. 19185–19189, https://doi.org/10.1073/pnas.1012833107.

Vasconcelos, C., and McKenzie, J.A., 1997, Microbial mediation of modern dolomite precipitation and diagenesis under anoxic conditions (Lagoa Vermelha, Rio de Janeiro, Brazil): Journal of Sedimentary Research, v. 67, p. 378–390, https://doi.org/10.1306/d4268577-2b26-11d7-8648000102c1865d.

Vasconcelos, C., McKenzie, J.A., Bernasconi, S., Grujic, D., and Tiens, A.J., 1995, Microbial mediation as a possible mechanism for natural dolomite formation at low temperatures: Nature, v. 377, p. 220–222, https://doi.org/10.1038/377220a0.

Wang, Y., Zhou, L., Zhao, L., Ji, M., and Gao, H., 2010, Palaeozoic uplands and unconformity in the North China block: Constraints from zircon LA-ICP-MS dating and geochemical analysis of bauxite: Terra Nova, v. 22, p. 264–273, https://doi.org/10.1111/j.1365-3121.2010.00942.x.

Weissberger, E.J., Coiro, L.L., and Davey, E.W., 2009, Effects of hypoxia on animal burrow construction and consequent effects on sediment redox profiles: Journal of Experimental Marine Biology and Ecology, v. 371, p. 60–67, https://doi.org/10.1016/j.jembe.2009.01.005.

Wells, A.J., 1962, Recent dolomite in the Persian Gulf: Nature, v. 194, p. 274, https://doi.org/10.1038/194274a0.

Whiteside, J.H., and Grice, K., 2016, Biomarker records associated with mass extinction events: Annual Review of Earth and Planetary Sciences, v. 44, p. 581–612, https://doi.org/10.1146/annurev-earth-060115-012501.

Wignall, P.B., and Twitchett, R.J., 2002, Extent, duration, and nature of the Permian-Triassic superanoxic event, in Koeberl, C., and MacLeod, K.G., eds., Catastrophic Events and Mass Extinctions: Impacts and Beyond: Geological Society of America Special Paper 356, p. 395–413, https://doi.org/10.1130/0-8137-2356-6.395.

Wright, D.T., and Wacey, D., 2005, Precipitation of dolomite using sulphate-reducing bacteria from the Coorong region, South Australia: Significance and implications: Sedimentology, v. 52, p. 987–1008, https://doi.org/10.1111/j.1365-3091.2005.00732.x.

Zhang, F., Xu, H., Konishi, H., Kemp, J.M., Roden, E.E., and Shen, Z., 2012, Dissolved sulfide-catalyzed precipitation of disordered dolomite: Implications for the formation mechanism of sedimentary dolomite: Geochimica et Cosmochimica Acta, v. 97, p. 148–165, https://doi.org/10.1016/j.gca.2012.09.008.

Printed in USA